

**Momčilović Nikola**

Assistant Professor  
University of Belgrade  
Faculty of Mechanical Engineering  
Serbia

**Motok Milorad**

Full Professor  
University of Belgrade  
Faculty of Mechanical Engineering  
Serbia

**Maneski Taško**

Full Professor  
University of Belgrade  
Faculty of Mechanical Engineering  
Serbia

# Hot Spot Along Corner Curvature of Rectangular Plate Opening

*Development of stress concentration in the corner zone of rectangular plate opening is a well-known fact. It is usually literally taken that the largest stress concentration factor (SCF) occurs exactly in the corner (at angle coordinate of 45 degrees in case of square opening). More rigorous analyses, however, reveal that this is not perfectly true. Although maximum stress never really “leaves the corner”, for some hot-spot analyses, more scrupulous investigation of this phenomenon has significance. In this paper, results of some analytical, numerical and experimental investigations of this topic, for plate in tension, are presented and compared.*

**Keywords:** stress concentration factor, hot spot, plate opening, corner radius of curvature, conformal mapping, FEM, digital image correlation, Aramis system.

## 1. INTRODUCTION

High stress concentration factor in the corner of the rectangular plate opening is a notorious fact. Due to that, openings in virtually all steel structures are made with rounded corners. Even when corner curvature is not fabricated on purpose, extreme stresses lead to plastic deformation and hence force a rounding.

It is usually literally taken that the largest stress occurs exactly in the corner (i.e. at angle coordinate of 45 degrees in case of square opening). Although more rigorous analyses reveal that this is not perfectly true, in vast majority of structural design tasks it is not necessary to scrutinize this phenomenon further. However, in some cases (hot-spot approach in FEM fatigue analyses, calibration of micro and nano pressure gauges) a closer look on the corner curvature itself may be of importance.

Stress field around a hole of thin orthotropic lamina is analyzed in [1]. Using complex variable method, the stress functions around the hole are obtained depending on material anisotropy, shape of the hole and loadings. In [2] least square boundary collocation method is used for the same purpose. Furthermore, a generalized Schwarz–Christoffel mapping function is employed to map the rectangular hole to a unit circular hole. Location of maximum stress is found to be in a wide range considering lamina arrangements. Paper [3] performed the similar analysis at the corners of polygonal hole of the finite plate. Finite element method and conformal method are used to obtain stress field around an opening in [4]. Paper showed that maximum stress point is not on the 45 degrees radii, but to some extent allocated. Furthermore, an application of finite element method in biaxial loading of plate with elliptic [5] and circular hole [6] is also investigated. A stress analysis

distribution around the hole of the composite plate and high stress concentration assessments in general could be also found in [7-12, 13-16].

Analytical analyses of this topic used in the paper are briefly summarized in Chapter 2. Numerical (finite element) analyses and experimental investigation of the same issue is described in Chapters 3&4 respectively. Results of all are presented in diagrams in Chapter 5.

## 2. ANALYTICAL SOLUTION

The key obstacle in applying analytical approach in problems of the kind is the lack of mathematical description of the contour of the opening. Square or rectangle with rounded corners cannot be presented analytically in a closed form. The problem can be solved using conformal mapping but, in further stress analyses, this demands the use of complex presentation of basic equations of the theory of elasticity. Thorough presentation of such approach, leading to analytical solutions for stresses on the contour of rectangular opening in infinite plate exposed to unidirectional in-plane tension, is given in [17] and [18]. It is based on early works of Muskhelishvili [19] and Savin [20]. Brief summary of those is given as follows.

The function of a complex variable  $\omega(\xi)$  for mapping a unit circle into square, rectangular, hexagonal etc. contours can be derived from the Schwarz - Christoffel integral in the form of infinite series:

$$\omega(\xi) = \sum_{i=-1,1}^{n=\infty} W_i \xi^i = W_{-1} \xi^{-1} + W_1 \xi^1 + W_3 \xi^3 + \dots + W_n \xi^n \quad (1)$$

$$W_{-1}=1; W_{qb-1} = \frac{(-1)^q \prod_{j=1}^{q-1} (jb-2)}{\frac{q!}{2} b^q (qb-1)}; q=1,2,3\dots \quad (2)$$

where  $b$  denotes the number of sides of the polygon.

Using complete series (1), i.e. infinite numbers of their terms, mapped contours achieve the shapes of regular polygons – with straight sides and no curvature in corners. Decreasing the number of terms in (1) used

Received: March 2019, Accepted: May 2019  
Correspondence to: Dr Milorad Motok, Full Professor,  
Faculty of Mechanical Engineering, Kraljice Marije 16,  
11120 Belgrade 35, Serbia  
E-mail: mmotok@mas.bg.ac.rs  
**doi:10.5937/fmet1904846M**

© Faculty of Mechanical Engineering, Belgrade. All rights reserved

FME Transactions (2019) 47, 846-850 **846**

in mapping (finite  $n$ ) one gets contours of curvilinear polygons. The radius of curvature of sides and corners is greater as the number of used terms in (1) is smaller. Putting  $b = 4$  and limiting  $4q-1 = n$ , for  $n = -1, 1, 3 \dots$ , a series of square “ $n$ -contours” is obtained with decreasing corner (and side) radii of curvature as the corresponding  $n$  is increasing (Fig. 1).

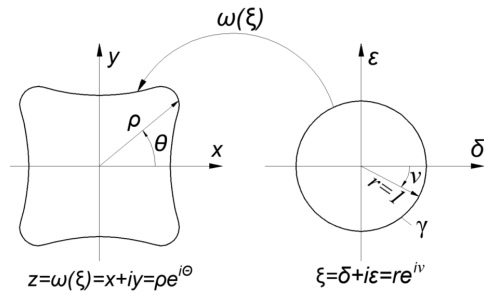


Figure 1. Mapping unit circle into a square

Thus, using appropriate  $n$ , contours of an arbitrary small corner radius of curvature can be analyzed. However, the introduction of complex variable demands the use of basic equations of theory of elasticity in complex form. This involves rather complicated mathematical apparatus in further stress evaluation which can be brought to a programmable and practically applicable shape only after transformations explained in [17]. Finally, it leads to expression for normal stress in a point on the contour in direction orthogonal to its radius:

$$\theta\theta = \frac{4 \sum_{k=0,2}^{n+1} \sum_{i=-1,1}^n F_i [i(i-k)] W_{i-k} + \Omega_k i(i+k) W_{i+k} \cos(kv)}{\sum_{k=0,2}^{n+1} \sum_{i=-1,1}^n W_i [i(i-k)] W_{i-k} + \Omega_k i(i+k) W_{i+k} \cos(kv)} \quad (3)$$

where  $\Omega = 0$  for  $k = 0$  and  $\Omega = 1$  for  $k \neq 0$ ; algorithm for computation of coefficients  $F_i$  is rather demanding and can be found in [1]. Upon value of  $\theta\theta$ , a principal  $S1$  stress in the point can be derived as:

$$S1 = \frac{\theta\theta}{\cos^2 \beta} \quad (4)$$

where the angle  $\beta$  is the difference between  $(\pi/2 - \theta)$  and the angle the tangent on the contour at the point forms with  $x$  - axis. Those are used for determination of SCF in proceeding.

Now consider a square,  $a \times a$ , opening, with corner radii  $R$ , in infinite plate exposed to tension in direction  $\theta = 0$  (Fig. 2). For largest corner radius  $R = a/2$ , square contour of the opening turns into a full circle with extreme stress concentration factor  $SCF = 3$  at  $\theta = \pi/2$ . (SCF is taken as the ratio of principle stress in a point and nominal tension applied to a plate). For  $R = 0$  virtually infinite stress develops at  $\theta = \pi/4$ . Results for in-between values of  $a/R$ , from 2 to 1500, calculated according to 2.2 ÷ 2.4 are presented in Table 1 and Figs. 5&6 in Chapter 5.

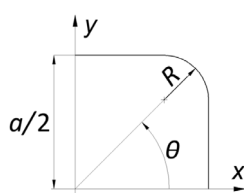


Figure 2. Quadrant of rectangular opening with rounded corner

### 3. NUMERICAL ANALYSES

Finite element method (FEM) is used as a numerical tool to determine locus of the maximum stress, as well as the exact value of SCF. FEM presents the most applied instrument to obtain stress, strain and displacement fields in the areas of geometric discontinuities, such are in this case, openings with small radii of curvature in their corners.

FE models used in this research replicate the experimental installation, fully described in following Chapter 4. Each presents a plate weakened by a rectangular opening with different corner radius of curvature. Numerical models expand a way over experimental tests, and are in range of radii between 0.2 mm and 50 mm.

Typical FE model consists of 25010 nodes and 25041 general purpose 4-node plate elements. Very fine mesh is generated in the zone of the radius. The corner radius is divided by 20 elements. SCF values convergence is already obtained using the 8-10 divisions, but in order to find the exact hot spot locus, denser mesh seems to be more appropriate (Fig. 3). Plate is subjected to axial tension of 29.6 kN.

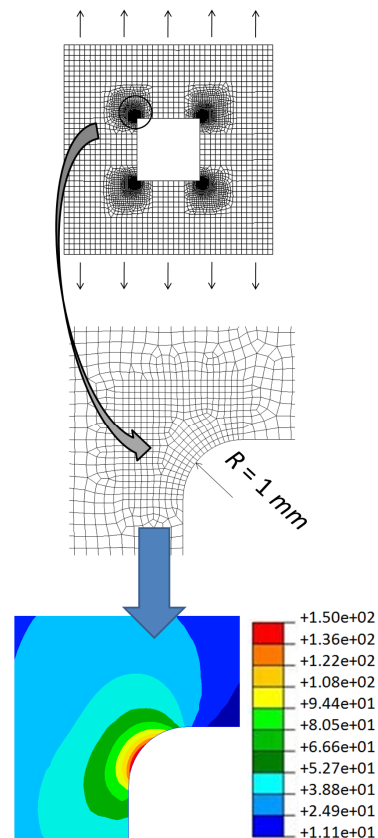


Figure 3. FEM Model, principal stress

### 4. EXPERIMENTAL INVESTIGATION

Principal stress field is obtained using DIC method (Digital Image Correlation). DIC can measure and graphically present displacement, strain and stress field on any surface under applied load. Unlike conventional measuring devices (strain gauges) DIC field gradient, locates stress concentration in such small

areas where classical devices could not be practically installed. This non-contact method records a non deformed surface and deformed surface under known loads [21-23]. By comparing the change in the point – the point distance in deformed and non deformed surface, it calculates displacement, and consequently strain and stress in each recorded point. Aramis system, which is based on DIC method, has a pair of cameras and a computer unit. Cameras record the experiment procedure and software calculates displacement based on the camera signal.

The most important part of the experiment is camera calibration. Calibration is extremely sensitive and can influence final results. Calibration procedure records several images based on prepared calibration panel in order to define measuring volume, optimal distance between cameras, range, proper illumination etc. Measuring surface has to be sprayed in order to create black dots on whitened surface. Cameras track these dots and their moving. Dots are divided into the pixels. Pixel size governs the quality of stress field change. The same analogy can be used as in the case of element size in finite element analyses.

Equipment consists of DIC based system, load cell and 1000 x 1000 x 3mm steel plate subjected to tension by hydraulic cylinder. Plate opening is rectangularly shaped (300 x 300 mm) with the following radii on its corners: 0.5 mm, 1 mm, 2 mm, 3 mm. Equipment installation and Aramis scheme are as shown on Fig. 4. Moreover, the figure presents DIC obtained locus of maximum principal stress around the 1 mm radius of curvature, for the axial tension of 29.6 kN.

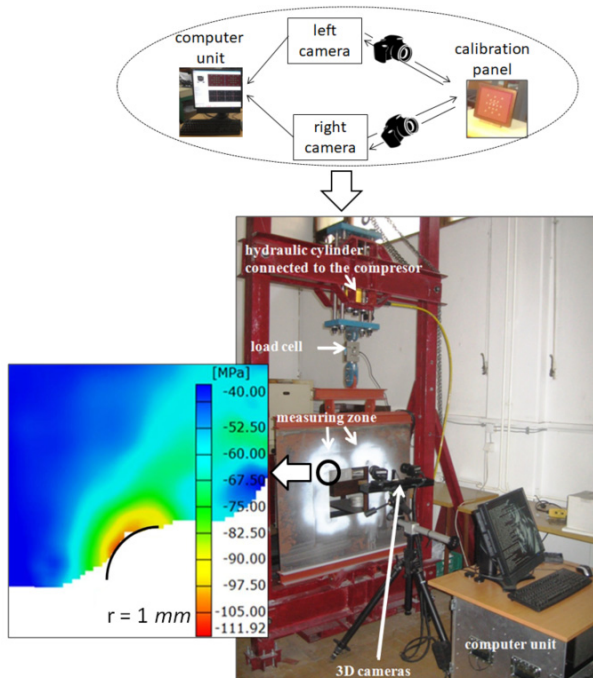


Figure 4. Experiment scheme and equipment

## 5. SUMMARY AND COMPARISON OF RESULTS

Results obtained analytically are summarized in Table 1 and graphically presented in inverted diagrams on Figs. 5&6. Equations of corresponding fitting curves are given in (5) and (6). Results obtained by FEM and

measurement are added in diagrams on Figs. 5&6 as dots, without fitting.

Table 1. Analytical results

SCFmax	$\theta$ (SCFmax)	a/R
4.4	52.47	16.67
6.0	49.16	40.86
7.3	47.81	70.35
8.5	47.09	105.46
9.6	46.64	144.50
10.6	46.33	187.86
11.6	46.11	234.51
12.5	45.95	284.79
13.3	45.82	337.97
14.2	45.72	394.33
15.0	45.64	453.31
15.8	45.57	515.16
16.5	45.52	579.42
17.3	45.47	646.30
18.0	45.43	715.44
18.7	45.39	787.01
19.4	45.36	860.70
20.1	45.34	936.67
20.8	45.31	1014.64
21.5	45.29	1094.77
22.1	45.27	1176.80
22.8	45.25	1260.88
23.4	45.24	1346.78
24.0	45.23	1434.64
24.7	45.21	1524.25

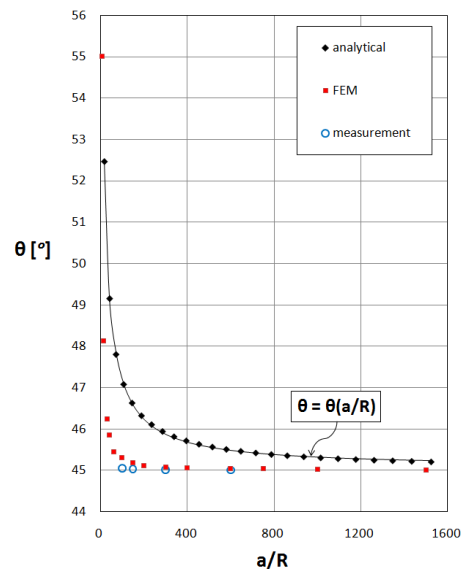


Figure 5.  $\theta$  (SCFmax) - a/R

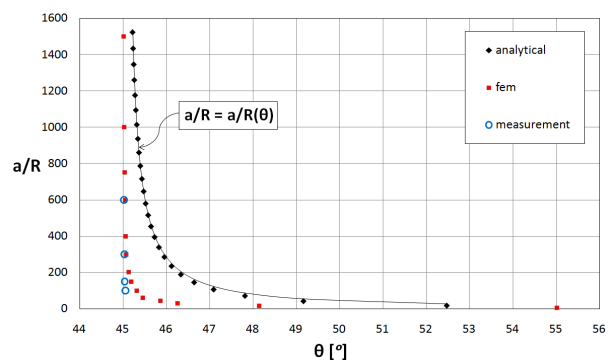


Figure 6. a/R -  $\theta$  (SCFmax)

The equations of fitting curves for analytical results in Figs. 5&6 read:

$$\theta = 45.0773 + \frac{40986.5}{\left(\frac{a}{R}\right)^3} - \frac{4654.84}{\left(\frac{a}{R}\right)^2} + \frac{254.92}{R} \quad (5)$$

$$\frac{a}{R} = \frac{\theta + \theta^2}{(\theta - 45.023)(\theta - 38.112)} \quad (6)$$

Analytical and FEM results differ in absolute values of  $\theta$  (SCFmax) from 0.5 degrees for smallest of investigated radii to 4.5 degrees for the largest. In most cases the difference is less than 2 degrees. Nevertheless, they clearly follow the same (hyperbolic) trend, but show some value difference.

Experiments are limited to only four different corner radii and, due to system sensitivity, were unable to perfectly match the numerical and FEM investigations. Nevertheless they undoubtedly follow the same trend.

## 6. CONCLUSION

In this paper, the precise location of maximum SCF along the corner curvature of rectangular plate opening is scrutinized. Analytical, numerical and experimental investigations reveal that hot-spot position generally differs from straightforwardly foreseen exact corner point (angle coordinate of 45 degrees in the case of a square opening). Although the decline from the very corner is generally small, for some aspects of design of such structures (fatigue) it might be significant.

Analytically, numerically and experimentally obtained results for the set of appropriate models are presented. Although analytical and numerical results follow the same trend (quasi-analytical expression of which fitting curve equation is given), it has to be noted that they differ qualitatively. Furthermore, strictly speaking, experimental results could not completely confirm the trends and hot spot allocation, since Aramis presented larger deviation from analytical and numerical approach. This can be associated with DIC sensitivity to exceptionally small measuring area, exploiting the Aramis system to its limits of application in which high stress gradients could not be fairly acquired within 1mm range.

## ACKNOWLEDGMENT

This work was supported by Ministry of Education, Science and Technological Development (Project no. TR 35009) of Serbia.

## REFERENCES

- [1] Dave J.M., Sharma D.S.: Stress Field Around Rectangular Hole in a Functionally Graded Plate, *International Journal of Mechanical Sciences*, Vol. 136, pp. 36 - 370, 2018.
- [2] Chauhan M. M., Sharma D.: Stresses in Finite Anisotropic Plate Weakened by Rectangular Hole, *International Journal of Mechanical Sciences*, Vol. 101-102, pp. 272-279, 2015.
- [3] Chauhan M. M., Sharma D.: Stress Concentration at the Corners of Polygonal Hole in Finite Plate, *Aerospace Science and Technology*, Vol. 58, pp. 197-206, 2016.
- [4] Louhghalam A., Igusa T., Park C., Choi S. and Kim K.: Analysis of Stress Concentrations in Plates with Rectangular Openings by a Combined Conformal Mapping – Finite Element Approach, *The International Journal of Solids and Structures*, Vol. 48, pp. 1991–2004, 2011.
- [5] Enab T.A.: Stress Concentration Analysis in Functionally Graded Plates with Elliptic Holes under Biaxial Loadings, *Ain Shams Engineering Journal*, Vol. 5, pp. 839 – 850, 2014.
- [6] Kumari S., Uphadhyay A.K. and Shukla K.K.: Stress Analysis for an Infinite Plate with Circular Holes, *5th International Conference on Materials Processing and Characterization, Proceedings 4*, pp. 2323-2332, 2017.
- [7] Rezaeepazhand J. and Jafari M.: Stress Analysis of Composite Plates with a Quasi-square Cut-out Subjected to Uniaxial Tension, *Journal of Reinforced Plastics and Composites*, Vol. 29, No. 13, pp. 2015–2026, 2010.
- [8] Sharma D.S.: Stress Distribution Around Polygonal Holes, *The International Journal of Mechanical Sciences*, Vol. 65, No. 1, pp. 115–24, 2012.
- [9] Yang Y., Liu J., Cai C.: Analytical Solutions to Stress Concentration Problem in Plate Containing Rectangular Hole under Biaxial Tension, *Acta Mechanica Sinica*, Vol. 21, No. 5, pp. 411–19, 2008.
- [10] Romeo G.: Analytical and Experimental Behaviour of Laminated Panels with Rectangular Opening under Biaxial Tension, Compression and Shear Loads, *Journal of Composite Materials*, Vol. 35, No. 8, pp. 639–64, 2001.
- [11] Rao D.K.N., Ramesh Babu M., Reddy K.R.N. and Sunil D.: Stress around square and rectangular cut-outs in symmetric laminates, *Composite Structures*, Vol. 92, pp. 2845–59, 2010.
- [12] Sharma D.S.: Stress Analysis of Infinite Laminated Composite Plate with a Polygonal Hole, *European Journal of Mechanics - A/Solids*, Vol. 54, pp. 44–52, 2015.
- [13] Momčilović N., Motok M. And Maneski T.: Stress Concentration on the Contour of a Plate Opening: Analytical, Numerical and Experimental Approach, *Journal of Theoretical and Applied Mechanics*, Vol. 51, pp. 1003-1012, 2013.
- [14] Maneski T., Bajić D., Momčilović N., Milošević Mitić V. and Balać M.: Determination of Internal Pressure Value Causing Pipe Branch Model to Plastically Deform, *FME Transaction*, Vol. 46, pp. 218-223, , 2018.
- [15] Kastratović G., Vidanović N., Grbović A. and Rašuo B.: Approximate Determination of Stress Intensity Factor for Multiple Surface Cracks, *FME transactions*, Vol. 46, pp. 39-45, 2018.
- [16] Perić M., Tonković Z., Maksimović K.S. Stamenković D.: Numerical Analysis of Residual Stre-

esses in a T-Joint Fillet Weld Using a Submodeling Technique, FME Transactions, Vol. 47, pp. 183-189, 2019.

- [17] Motok M.: Stress Concentration on the Contour of the Plate Opening of an Arbitrary Corner Radius of Curvature, Marine Structures, Vol.1, No.1, pp. 1-13, 1997.
- [18] Motok M.: Locus of the Maximum Stress in the Rounded Corner Zone of the Plate Opening, Transactions, Vol. 26, Issue 1, pp. 38-39, 1997.
- [19] Muskhelishvili N.I.: *Some Basic Problems of the Mathematical Theory of Elasticity*, P. Noordhoff, 1953.
- [20] Savin G.N.: *Stress Concentration Around Holes*, Pergamon Press, 1961.
- [21] Sutton M.: Digital image correlation for shape and deformation measurements, Handbook of experimental solid mechanics, pp. 565-600, 2008.
- [22] Hild F., Roux S.: Digital Image Correlation: from Displacement Measurement to Identification of Elastic Properties – a Review, Strain, Vol. 42, No. 2, pp. 69-80, 2006.
- [23] Fazzini M., Mistou S., Dalverny O., Robert L.: Study of image characteristics on digital image correlation error assessment, Optics and Lasers in Engineering, Vol. 48, pp. 335-339, 2010.

#### NOMENCLATURE

$\omega(\xi)$	mapping function
$\xi = \delta + i\varepsilon$	complex variable
$\theta$	angle coordinate (measured from $x$

– axes in anti-clock-wise direction)  
normal stress in a point on the contour in direction orthogonal to its radius  
 $R$  corner radius of curvature  
 $SI$  principle stress in a point on the contour  
 $XX$  nominal tension stress applied to plate in  $x$  – direction  
 $SCF = SI/XX$  stress concentration factor  
 $a$  rectangle side length

---

#### ТАЧКА НАЈВЕЋЕГ НАПОНА НА КОНТУРИ КВАДРАТНОГ ОТВОРА У ПЛОЧИ

Н. Момчиловић, М. Моток, Т. Манески

Концентрација напона у углу квадратног отвора у плочи је позната чињеница. Најчешће се узима да је највећа концентрација напона у самом темену угла (на угаоној координати од 45 степени у случају квадратног отвора). Ригорозније анализе, ипак, приказују да ово баш није најтачније. Иако максимални напон никада „не напушта“ угао, у неким прорачунима концентрације напона, озбиљније анализе овог феномена добијају на значају. У овом раду приказани су и поређени резултати аналитичке, нумеричке и експерименталне анализе тачне позиције концентрације напона у углу отвора, у случају плоче при истезању.